Draft 11 June 1999, to be submitted to Astrophysical Journal Letters
Preprint typeset using LaTeX style emulateapj

A MEASUREMENT OF THE ANGULAR POWER SPECTRUM OF THE CMB FROM $\ell = 100$ TO 400

A. D. Miller[1], R. Caldwell[1,2], M. J. Devlin[2], W. B. Dorwart[1], T. Herbig[1], M. R. Nolta[1], L. A. Page[1], J. Puchalla[2], E. Torbet[1], H. T. Tran[1]

Draft 11 June 1999, to be submitted to Astrophysical Journal Letters

ABSTRACT

We report on a measurement of the angular spectrum of the CMB between $l \approx 100$ and $l \approx 400$ made at 144 GHz from Cerro Toco in the Chilean Altiplano. When the new data are combined with previous data at 30 and 40 GHz, taken with the same instrument observing the same section of sky, we find: 1) a rise in the angular spectrum to a maximum with $\delta T_l \approx 85\ \mu$K at $l \approx 200$ and a fall at $l > 300$, thereby localizing the peak near $l \approx 200$; and 2) that the anisotropy at $l \approx 200$ has the spectrum of the CMB.

Subject headings: cosmic microwave background—cosmology

1. INTRODUCTION

It is widely recognized that the characterization of the cosmic microwave background (CMB) anisotropy is essential for understanding the process of cosmic structure formation (e.g. Hu et al. 1997, Bennett et al. 1997, Turner & Tyson 1999). If some of the currently popular models prove correct, the anisotropy may be used to strongly constrain cosmological parameters (e.g. Jungman et al. 1995, Bond et al. 1998). Summaries of the state of our knowledge of the CMB (e.g. Bond et al. 1998b (BJK), Page & Wilkinson 1999) suggest the existence of a peak in the angular spectrum near $l = 200$. In particular, BJK show $150 \leq l_{peak} \leq 350$. Since their analysis there have been additional results at $l > 200$ that lend support to their picture (Baker et al. 1999 (CAT), Glanz 1999 (VIPER), Wilson et al. 1999 (MSAM)). Here, we report the results from the *TOCO98* campaign of the Mobile Anisotropy Telescope (*MAT*) which probes from $l \approx 100$ to $l \approx 400$.

2. INSTRUMENT

The *MAT* telescope, based on the design in Wollack et al. 1997, is described briefly in Torbet et al. 1999 and Devlin et al. 1998 and is documented on the web[3]. In this paper, we focus on results from the two D-band (144 GHz) channels. The receivers use SIS mixers designed and fabricated by A.R. Kerr and S.-K. Pan of NRAO (National Radio Astronomy Observatory) and A.W. Lichtenberger of the University of Virginia (Kerr et al. 1993). The six other detectors in the focal plane are 30 and 40 GHz high electron mobility transistor (HEMT) amplifiers designed by M. Pospieszalski (Pospieszalski 1992, Pospieszalski et al. 1994).

The mixers, which operate in double sideband mode, are fed with a 25% bandwidth corrugated feed cooled to 4.5 K. The 144 GHz local oscillator (LO) is cavity stabilized and thermally controlled. The cryogenic IF HEMT amplifier, which operates between 4 and 6 GHz, is also of NRAO design. The resultant passband has been measured (Robertson 1996) to be approximately 138-140 and 148-150 GHz. The total system sensitivity (including atmospheric loading) for each receiver is ≈ 1.3 mK s$^{1/2}$ (Rayleigh-Jeans) with the SIS body operating at ≈ 4.4 K.

The $D1$ feed ($az = 207^\circ\!.47$, $el = 40^\circ\!.63$) is near the center of the focal plane, resulting in $\theta_{\rm FWHM} \approx 0^\circ\!.2$ ($\Omega_{\rm D1} = 1.36 \times 10^{-5}$ sr) while $D2$ is displaced from the center by 2.9 cm ($az = 205^\circ\!.73$, $el = 40^\circ\!.13$), resulting in $\theta_{\rm FWHM} \approx 0^\circ\!.3$ ($\Omega_{\rm D2} = 2.93 \times 10^{-5}$ sr). $D1$ is polarized with the E-field in the horizontal direction and $D2$ with the field in the vertical direction. No use is made of the polarization information in this analysis.

In the 1997 campaign (Torbet et al. 1999), a microphonic coupling rendered the D-band data suspect. The problem was traced to a combination of the azimuth drive motor and the chopper. The coupling was effectively eliminated for the 1998 campaign. In addition, the chopper amplitude was reduced from $2^\circ\!.96$ to $2^\circ\!.02$ and the frequency reduced from 4.6 Hz to 3.7 Hz. In all other respects, the instrument was the same as for 1997.

The telescope pointing is established through observations of Jupiter and is monitored with two redundant encoders on both the azimuth bearing and on the chopper. The absolute errors in azimuth and elevation are $0^\circ\!.04$, and the relative errors are $<0^\circ\!.01$. The chopper position, which is calibrated in the field, is sampled 80 times per chop. When its *rms* position over one cycle deviates more than $0^\circ\!.015$ from the average position (due to wind loading), we reject the data.

The analysis uses data between 20 and 200 Hz. These frequencies are well removed from the refrigerator cycle frequency at 1.2 Hz, the chopper frequency, and the Nyquist frequency at 592 Hz. The amplitude of the electronic transfer function varies by $< 2\%$ over this band.

3. OBSERVATIONS AND CALIBRATION

Data were taken at a 5200 m site[4] on the side of Cerro Toco (lat. = -22$^\circ\!.$95, long. = 67$^\circ\!.$775), near San Pedro de Atacama, Chile, from Aug. 26, 1998 to Dec. 7, 1998. For the anisotropy data, the primary optical axis is fixed

[1]Princeton University, Physics Department, Jadwin Hall, Princeton, NJ 08544

[2]University of Pennsylvania, Department of Physics and Astronomy, David Rittenhouse Laboratory, Philadelphia, PA 19104

[3]Details of the experiment, synthesis vectors, likelihoods, data, and analysis code may be found at http://www.hep.upenn.edu/CBR/ and http://physics.princeton.edu/~cmb

[4]The Cerro Toco site of the Universidad Católica de Chile was made available through the generosity of Prof. Hernán Quintana, Dept. of Astronomy and Astrophysics. It is near the proposed MMA site.

at az = 207°.41, el = 40°.76, δ = -60°.9 and the chopper scans 6°.12 of sky. We present here the analysis of data from Sept. 3, 1998 to Oct. 28, 1998.

Jupiter is used to calibrate all channels and map the beams. Its brightness temperature is 170 K in D-band (Griffin et al. 1986, Ulich et al. 1981) and the intrinsic calibration error is 5%. We account for the variation in angular diameter. To convert to thermodynamic units relative to the CMB, we multiply by 1.67 ± 0.03. The error is due to incomplete knowledge of the passbands.

After determining the beam parameters from a global fit of the clear weather Jupiter calibrations, the standard deviation in the measured solid angle is 5.5% for D1 and 4% for D2. Jupiter is observed on average within 2 hours of the prime observing time (approximately 10 PM to 10 AM local). The responsivity varies $\approx$ 20% over two months. In all, there are $\approx$ 35 Jupiter calibrations in each channel.

To verify the calibration between observations of Jupiter, a 149 GHz tone is coupled to the detectors through the LO port for 40 msec every 100 seconds. Its effective temperature is $\approx$ 1 K. There is good long term agreement between the Jupiter and pulse calibrations. The short-term (< 1 day) calibration is determined with a fit of the pulses to the Jupiter calibrations. The measurement uncertainty in the calibration is 7%.

The total 1σ calibration error of 10% for $D1$ and 9% for $D2$ is obtained from the quadrature sum of the above sources. In the full analysis, $D1$ and $D2$ are combined; thus the uncorrelated component of the error adds in quadrature yielding an error for the combination of 8%.

4. DATA REDUCTION

The data reduction is similar to that of the *TOCO97* experiment (Torbet et al. 1999). We use the terminology discussed there and in Netterfield et al. 1997. For $D1$ we form the 2-pt through 16-pt synthesized beams and for $D2$, the 2-pt through 17-pt synthesized beams. In practice, atmospheric contamination precludes using the 2-pt through 4-pt data and the achieved sensitivity renders the 17-pt and higher uninteresting.

The phase of the time ordered data relative to the beam position is determined with observations of Jupiter and the Galaxy. In the analysis, we use the phase for each harmonic that obtains when the quadrature signal from the Galaxy is minimized.

A quantity useful in assessing sensitivity to the beam shape is $l_{\rm eff}\theta_{\rm FWHM}$. For *SK* at $l_{eff} = 256$, $l_{\rm eff}\theta_{\rm FWHM} = 2.5$. For *TOCO98* at $l = 415$, $l_{\rm eff}\theta_{\rm FWHM} = 1.5$ for $D1$ and 2.2 for $D2$. This corresponds to a separation of lobes in the synthesized beam of $2\theta_{\rm FWHM}$ for $D1$ and $1.3\theta_{\rm FWHM}$ for $D2$.

As with *TOCO97*, the harmonics are binned according to the right ascension at the center of the chopper sweep. The number of bins depends on the band and harmonic as shown in Table 1. For each night, we compute the variance and mean of the data corresponding to a bin. These numbers are averaged over the 25 good nights and used in the likelihood analysis.

After cuts based on pointing, the data are selected according to the weather. For each n-pt data set, we find the mean *rms* of 6.5 sec averages over each 15 minute segment. When this value exceeds 1.2 of the minimum value for a given day, the data from that 15 min segment, along with the previous and subsequent 15 min segments are cut. The effect is to keep 5-10 hour blocks of continuous good data in any day, and to eliminate transitions into periods of poor atmospheric stability. Increasing the cut level adds data to the beginning and end of the prime observing time.

The stability of the instrument is assessed through internal consistency checks and we examine it with the distribution of the offset of each harmonic. The offset is the average of a night of data after the cuts have been applied (the duration ranges from 5-10 hours) and is typically of magnitude $\approx$ 150 μK with standard deviation $\approx$ 75 μK. The offsets for these data were stable over the campaign. The resulting χ^2/ν is typically $1-4$. For the offsets of the quadrature signal, χ^2/ν is typically $1-2$. The stability of the offset led to a relatively straightforward data reduction.

To eliminate the potential effect of slow variations in offset, we remove the slope and mean for each night for each harmonic. This is accounted for in the quoted result following Bond et al. 1991.

5. ANALYSIS AND DISCUSSION

In the analysis, we include all known correlations inherent in the observing strategy. In computing the "theory covariance matrix" (BJK) which encodes the observing strategy, we use the measured two dimensional beam profiles. From the data, we determine the correlations between harmonics due to the atmosphere. Because the S/N is only $2-5$ per synthesized beam, and the noise is correlated between beams, we work with groups of harmonics. This is similar to band averaging, though we use the full covariance matrix so as to include all correlations.

Table 1 gives the results of separate analyses of $D1$ and $D2$. Both channels show a fall in the angular spectrum above $l = 300$. The fact that the results agree is an important check as the receivers (other than the optics) are independent. It is not possible to compute $D1-D2$ directly from the data because of the different beam sizes. The eventual production of a map will facilitate the comparison.

In the full analysis, $D1$ and $D2$ are combined. The resulting likelihoods are shown in Figure 1 along with the results of the null tests. Because $D1$ and $D2$ observe the same section of sky at different times, some care must be taken in computing the correlation matrices. The correlation coefficients between $D1$ and $D2$ due to the atmosphere are of order 0.05. The largest off-diagonal terms of the theory covariance matrix are $\lesssim 0.4$ The quoted results are insensitive to the precise values of the off-diagonal terms of the covariance matrix. The combined analysis affirms what is seen in $D1$ and $D2$ individually and shows a peak in the angular spectrum near $l = 200$.

The *TOCO98* data agree with the *TOCO97* data in the regions of common l. We compute the spectral index of the fluctuations by comparing band powers. We find $\beta_{CMB} = \ln(\delta T_{144}/\delta T_{36.5})/\ln(144/36.5) = -0.04 \pm 0.25$, (including calibration error), where δT_{144} is the weighted mean of the two highest points for *TOCO98* and $\delta T_{36.5}$ is a similar quantity for *TOCO97* (36.5 GHz is the average *TOCO97* frequency). For the CMB, $\beta_{CMB} = 0$. For dust, $\beta_{RJ} = 1.7$ corresponds to $\beta_{CMB} = 2.05$; for free-free emission $\beta_{RJ} = -2.1$ corresponds to $\beta_{CMB} = -1.75$. Though it is possible for spinning dust grains (Drain & Lazarian 1999)

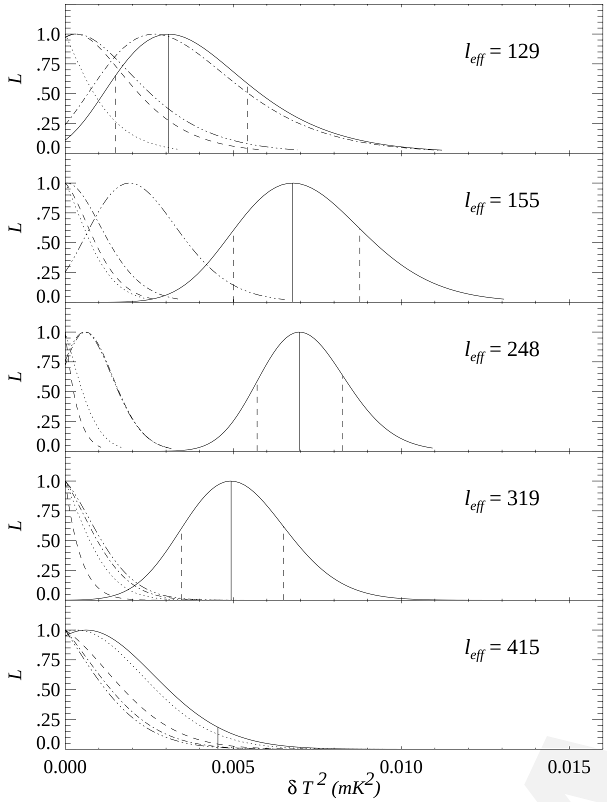

FIG. 1.— The likelihood of the combined $D1$ and $D2$ analysis (solid line) as a function of δT_l^2. The null tests: quadrature (signal with chopper sweeping one direction minus that with the chopper sweeping the other direction, dotted line), fast and slow dither (differences of subsequent 0.5s and 10s averages, dash and dash-dot lines respectively) and first half minus second half (dot-dot-dot-dash line), are also shown. The vertical lines indicate the maximum, $\pm\ 1\sigma$, or 95% confidence upper bound.

to mimic this spectrum for our frequencies, the amplitude of this component is small (de Oliveira-Costa et al. 1998). In addition, the spatial spectrum of diffuse sources like interstellar dust falls as $l^{-3/2}$ (Gautier et al. 1992), so the observed peak is inconsistent with our observations at $l \approx 100$.

The frequency spectral index of unresolved extra-Galactic sources is typically $\beta_{RJ} = -2$ to -3, inconsistent with the measured index. In addition, the spatial spectrum of sources rises as $\delta T_l \propto l$, inconsistent with our observations at $l = 400$. Moreover, recent analyses (e.g. Tegmark 1999) estimate the level of point source contamination to be much lower than the fluctuations we observe. We therefore conclude that the source of the fluctuations is the CMB.

We assess the statistical significance of the decrease in δT_l for $l > 300$ by comparing just the likelihood distributions at $l = 248$ (L_{248}), for which $\delta T_l = 83\ \mu$K, and $l = 415$, for which $\delta T_l < 68\ \mu$K (95%). These two distributions are effectively uncorrelated. The integral of the area normalized likelihood of L_{415} for values of δT^2 below which $L_{415} = L_{248}$ is 0.95; this is the probability that $\delta T_{415} < \delta T_{248}$. The point at which $L_{415} = L_{248}$ is also coincidentally the 2σ lower limit on δT_{248} and the 95% upper limit on δT_{415}. The probability that $\delta T_{415} \leq 83\ \mu$K (the peak of L_{248}) is 0.996. When all the data in Figure 2

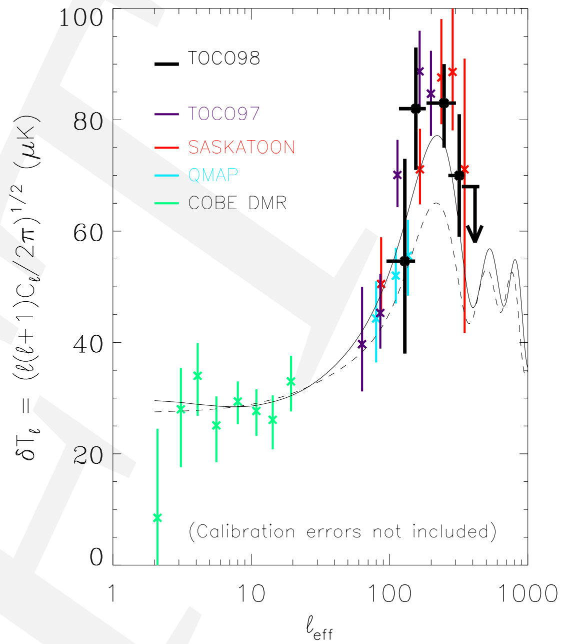

FIG. 2.— Angular spectrum from *COBE*/DMR, *SK*, *QMAP*, *TOCO97*, and *TOCO98* D-band. The *SK* data have been recalibrated according to Mason et al. 1999, leading to an increase of 5%, and reduced according to the foreground contribution in de Oliveira-Costa et al. 1997, leading to a reduction of 2% (*i.e.* a net 3% increase in the mean and 5% increase in the error bars over Netterfield et al. 1997). The revised *SK* calibration error is 11%. The *QMAP* data are the same as those reported in de Oliveira-Costa et al. 1998 and have an average calibration error of 12%. The correction for foreground emission is $\approx 2\%$, though it has not yet been precisely determined and so is not included. Both *SK* and *QMAP* are calibrated with respect to Cas-A. The *TOCO97* data, which have a calibration error of 10%, are calibrated with respect to Jupiter. The *TOCO98* data are shown with l-space bandwidth as the horizontal bars.The cosmological models are computed with CMBFAST (Seljak & Zaldarriaga 1998). The dashed line is "standard CDM" ($\Omega_m = 1$, $\Omega_b = 0.05$, $h = 0.5$) the solid line is a "concordance model" (Wang et al. 1999, Turner 1999) with $\Omega_m = 0.33$, $\Omega_b = 0.041$, $\Omega_\Lambda = 0.67$, and $h = 0.65$. For *COBE*/DMR we use Tegmark 1997. The error bars are "1σ statistical."

are considered, these probabilities will increase.

The weighted mean of data from *TOCO97*, *TOCO98*, and *SK* between $l = 150$ and 250, is $\delta\bar{T}_{\rm peak} = 82\ \pm 3.3 \pm 5.5\ \mu$K (the second error is calibration uncertainty). This is consistent with, though slightly higher than, the value from the Wang et al. 1999 concordance model plotted in Figure 2, which gives $\delta\bar{T}_{\rm peak} \approx 75\mu$K. In the context of this model, the high $\delta\bar{T}_{\rm peak}$ favors a smaller $\Omega_m h^2$ (e.g. larger "cosmological constant") or more baryons.

Figure 2 shows results taken over six years and seven observing campaigns and three different experiments. Though a detailed confrontation with cosmological models will have to await a thorough analysis and comparison with other experiments, a straightforward read of the data indicates a rise to $\delta\bar{T}_{\rm peak} \approx 85\ \mu$K at $l \approx 200$ and a fall at $l > 300$. The data strongly disfavor models with a peak in the spectrum at $l = 400$. Future work will include the analysis of the *TOCO98* HEMT and remaining D-band data.

We gratefully acknowledge conversations with and help from Dave Wilkinson, Norm Jarosik, Suzanne Staggs, Steve Myers, David Spergel, Angel Otárola, Hernán Quintana, the Princeton Machine Shop, Bernard Jones, Harvey Chapman, Stuart Bradley, and Eugenio Ortiz. The experiment would not have been possible without NRAO's site monitoring and detector development. We also thank Lucent Technologies for donating the radar trailer. This work was supported by an NSF NYI award, a Cottrell Award from the Research Corporation, a David and Lucile Packard Fellowship (to LP), a NASA GSRP fellowship to AM, an NSF graduate fellowship to MN, a NSF Career award (AST-9732960, to MD), NSF grants PHY-9222952, PHY-9600015, and the University of Pennsylvania. The data will be made public upon publication of this *Letter*.

REFERENCES

Baker, J.C., Grainge, K., Hobson, M.P., Jones, M.E., Kneissl, R., Lasenby, A.N., O'Sullivan, C.M.M., Pooley, G. Rocha, G., Saunders, R., Scott, P.F., Waldram, E.M. 1999, Submitted to MNRAS, astro-ph/9904415

Bennett, C. L. , Turner, M. S., White, M. 1997, Physics Today, 50:11:32

Bond, J. R., Efstathiou, G., Tegmark, M., Lubin, P.M., & Meinhold, P.R. 1991, Phys. Rev. Lett., 66, 2179

Bond, J. R. 1996 *Theory and Observations of the Cosmic Microwave Background Radiation*, in "Cosmology and Large-Scale Structure," Les Houches Session LX, August 1993, ed. R. Schaeffer, Elsevier Science Press

Bond, J. R., Efstathiou, G., Tegmark, M. 1998, MNRAS, 50, L33-41

Bond, J. R., Jaffe, A. H., Knox, L. 1999, Accepted in ApJ, astro-ph/9808264

de Oliveira-Costa, A., Kogut, A., Devlin, M. J., Netterfield, C. B., Page, L. A., Wollack, E. J. 1997 ApJ, 482:L17-L20

de Oliveira-Costa, A., Devlin, M. J., Herbig, T. H., Miller, A.D., Netterfield, C. B., Page, L. A. & Tegmark, M. 1998 ApJ, 509:L77

de Oliveira-Costa, A., Tegmark, M., Page, L.A., Boughn, S. 1998 ApJ, 509:L9

Devlin, M. J., de Oliveira-Costa, A., Herbig, T., Miller, A. D., Netterfield, C. B., Page, L. A., & Tegmark, M. 1998, ApJ, 509:L73

Drain, B. T. & Lazarian, A. 1999, astro-ph/9902356, in *Microwave Foregrounds*, ed A. de Oliveira-Costa & M. Tegmark (ASP:San Francisco)

Gautier, T. N. I., Boulanger, M., Perault, M., Puget, J. L. 1992, AJ, 103, 1313

Glanz, J. 1999. In the "News" section, Science, Vol 283. See also the VIPER web site at http://cmbr.phys.cmu.edu

Griffin, M. J., Ade, A. R., Orton, G. S., Robson, E. I., Gear, W.K., Nolt, I. G., and Radostitz, J. V. 1986, *Icarus*, 65, 244

Hu, W., Sugiyama, N., and Silk, J. 1997, Nature, 386,37

Jungman, G., Kamionkowski, M., Kosowsky, A., and Spergel, D. N. 1995, Phys. Rev. D., 54, 1332

Kerr, A. R., Pan, S. -K., Lichtenberger, A. W., and Lloyd, F. L. 1993, Proceedings of the Fourth International Symposium on Space Terahertz Technology, pp 1-10

Mason *et al.* 1999, astro-ph/9903383

Netterfield, C. B., Devlin, M. J., Jarosik, N., Page, L., & Wollack, E. J. 1997, ApJ, 474, 47

Page, L. and Wilkinson, D. T. 1999, Centenary Rev Mod Phys 71:S173

Pospieszalski, M. W. 1992, Proc. IEEE Microwave Theory Tech., MTT-3 1369; and Pospieszalski, M. W. 1997, Microwave Background Anisotropies, ed F. R. Bouchet (Gif-sur-Yvette: Editions Frontirres): 23-30

Pospieszalski, M. W. et al. 1994 IEEE MTT-S Digest 1345

Robertson, T.L., 1996. "Development of a 144 GHz Cryogenic Heterodyne Radiometer Based on SIS Junctions," Princeton Sr. Thesis (Adv. L. Page)

Seljak, U. and Zaldarriaga, M. 1998. The CMBFAST code is available through http://www.sns.ias.edu/matiasz/CMBFAST/cmbfast.html. See also 1996 ApJ469:437-444

Smoot, G.F., *et al.* 1992, ApJ396:L1

Tegmark, M. 1997, PRD, 55:5895

Tegmark, M., Eisenstein, D., Hu, W., & de Oliveira-Costa, A. 1999, Submitted to ApJ, astro-ph/9905257

Torbet, E., Devlin, M. J., Dorwart, W. Herbig, T., Nolta, Miller, A. D., Page, L., Puchalla, J., & Tran, H. 1999, ApJ, Submitted. See also astro-ph/9905100

Turner, M.S., 1999, astro-ph/9904051

Turner, M.S. and Tyson, J.A. 1999 Centenary Rev Mod Phys 71:S145

Ulich, B. L. 1981, *Astr. J.*, 86:11, 1619

Wang, L., Caldwell, R.R., Ostriker, J. P. & Steinhardt, P.J. 1999, astro-ph/9901388

Wilson, G. W., et al. 1999, Submitted to ApJ, astro-ph/9902047

Wollack, E. J., Devlin, M. J., Jarosik, N.J., Netterfield, C. B., Page, L., Wilkinson, D. 1997, ApJ, 476:440-447

TABLE 1
TOCO98 ANGULAR SPECTRUM

N_{bins} [a]	$D1$ n-pt	$D1$ $l_{\rm eff}$ [b]	$D1$ δT_l [c] μK	$D2$ n-pt	$D2$ $l_{\rm eff}$ [b]	$D2$ δT_l [c] μK	$D1$+$D2$ $l_{\rm eff}$ [b]	$D1$+$D2$ δT_l [c] μK
128(84)	...	...	...	5	129^{+24}_{-34}	55^{+18}_{-17}	129^{+24}_{-34}	55^{+18}_{-17}
128(84)	5,6	146^{+31}_{-40}	93^{+14}_{-12}	6	163^{+22}_{-39}	67^{+18}_{-17}	155^{+28}_{-38}	82^{+11}_{-11}
192(125)	7,8	223^{+23}_{-49}	86^{+13}_{-13}	7-10	257^{+46}_{-36}	86^{+9}_{-9}	248^{+54}_{-63}	83^{+7}_{-8}
256(165)	9-12	300^{+47}_{-75}	89^{+11}_{-11}	11,12	330^{+14}_{-55}	< 80 95%	319^{+28}_{-53}	70^{+11}_{-11}
384(250)	13-16	453^{+35}_{-76}	< 82 95%	13-17	399^{+2}_{-67}	< 82 95%	415^{+31}_{-82}	< 68 95%

NOTE— (a) The number of bins on the sky followed by, in parentheses, the number used in the analysis due to the galactic/atmosphere cut. (b) The range for $\ell_{\rm eff}$ denotes the range for which the window function exceeds $e^{-1/2}$ times the peak value. (c) The error on $\delta T_\ell = [\ell(\ell+1)C_\ell/2\pi]^{1/2}$ is comprised of experimental uncertainty and sample variance. The calibration error is **not** included.